ЖЭТФ, 2015, том 148, вып. 2 (8), стр. 299–303 © 2015

INVESTIGATION OF LOCAL TUNNELING CURRENT NOISE SPECTRA ON THE SILICON CRYSTAL SURFACES BY MEANS OF STM/STS

V. N. Mantsevich[a]*, *N. S. Maslova*[a], *G. Y. Cao*[b]

[a] *Lomonosov Moscow State University, Department of Physics 119991, Moscow, Russia*

[b] *Wuhan Institute of Physics and Mathematics, Chinese Academy of Sciences, China*

Received December 5, 2014

We report on a careful analysis of the local tunneling conductivity by means of ultra-high vacuum scanning tunneling microscopy/spectroscopy (STM/STS) technique in the vicinity of low-dimensional structures on the Si(111)–(7 × 7) and Si(110)–(16 × 2) surfaces. The power-law exponent α of low-frequency tunneling current noise spectra is investigated for different values of the tunneling contact parameters: relaxation rates, the localized state coupling, and the tunneling barrier width and height.

DOI: 10.7868/S004445101508012X

1. INTRODUCTION

Low-frequency noise with the spectral density $1/f^\alpha$ is a ubiquitous phenomenon, which hampers operations of many devices and circuits. The problem of low-frequency noise formation with a $1/f^\alpha$ spectrum in electron devices is one of the most interesting and important in recent years. Low-frequency noise was discovered for the first time in vacuum tubes [1] and later observed in a wide variety of electronic materials [2–4]. The importance of the low-frequency noise for electronic and communication devices gave rise to numerous studies of its physical mechanisms and methods for its control. However, after many years of investigation [5–8], the origin of $1/f^\alpha$ noise is still not clear. Up to now, the typical approach to the $1/f^\alpha$ noise problem consists in "by hand" introducing a random relaxation time τ for a two-state system with the probability distribution function A/τ_0^α. Therefore, the noise spectrum of a two-state system averaged over τ_0 has a power-law singularity. But the physical nature and microscopic origin of such a probability distribution function is unknown in general. Although the current noise gives a basic limitation for the performance of a scanning tunneling microscope, only a limited number of works were devoted to the study of $1/f^\alpha$ noise. Correspondingly, no comprehensive methods for low-frequency noise suppression in modern devices and especially in the tunneling contacts have been developed.

The scanning tunneling microscopy (STM) data obtained above the surface of pyrolytic graphite were analyzed in [9] and [10]. The power-low exponent α equal to about 1.4 was determined in [10]. The tunneling current noise spectrum in the vicinity of individual impurity atoms on an InAs(110) surface was investigated in [11] and it was revealed that the power-law exponent of $1/f^\alpha$ noise depends on the presence of an impurity atom in the tunneling junction area. The tunneling current noise at the zero value of applied bias voltage was investigated in [12]. Measurements were carried out at the ultra-high vacuum conditions at the base pressure $5 \cdot 10^{-11}$ Torr. It has been demonstrated that at the zero bias voltage, the $1/f^\alpha$ component of noise in the tunneling current vanishes and white noise becomes dominant. The physical phenomena that govern the $1/f^\alpha$ tunneling current noise fluctuations were discussed in [13–15]. Coulomb blockade as one of the sources of $1/f^\alpha$ noise formation was considered in [13]. Another possible mechanism is connected with the atomic adsorption/desorption processes on the sample/tip surface in the tunneling contact [14]. In [15], the $1/f^\alpha$ tunneling current noise was explained in terms of surface diffusion of adsorbed molecules in the tunneling contact area.

*E-mail: vmantsev@spmlab.phys.msu.su

Theoretical investigations of the noise in a two-level system was carried out in [16–19]. In [16], the authors studied current noise in a double-barrier resonant-tunneling structure due to dynamic defects that switch states because of their interaction with a heat bath. Time fluctuations of the resonant level result in low-frequency noise, which depends on the relative strengths of the electron escape rate and the defect switching rate. If the number of defects is large, the noise is of the $1/f$ type. In [17], the authors studied shot noise in a mesoscopic quantum resistor. They found correlation functions of all orders and the distribution function of the transmitted charge and considered the Pauli principle as the reason for the fluctuations. The current fluctuations in a mesoscopic conductor were studied in [18]. A general expression for fluctuations in a cylindrical tunneling contact in the presence of a time-dependent voltage was derived. In [19], the authors demonstrated that low-frequency tunneling current noise is the result of a sudden Coulomb-interaction switching on and off of conduction electrons with charged states localized in the tunneling contact.

To the best of our knowledge, tunneling current noise STM/STS (scanning tunneling spectroscopy) measurements have been performed only for relatively simple surfaces like those of gold, graphite, or graphene. In this paper, we report on detailed investigations of the low-frequency tunneling current noise spectrum in the vicinity of low-dimensional structures on the Si(111)–(7×7) and Si(110)–(16×2) surfaces. We payed special attention to the dependence of the power-law exponent α of the low-frequency tunneling current noise spectrum on the tunneling contact parameters: relaxation rates, the localized state coupling, and the tunneling barrier width and height. Decreasing low-frequency noise is a necessary and important task for performing precision measurements. During scanning tunneling microscopy experiments, we often deal with measurements in the presence of localized states. Hence, our main goal was to investigate low-frequency noise on surfaces, where localized states are formed by the low-dimensional surface structures, and to analyze the influence of system parameters (the tunneling current and the bias voltage) on the behavior of low-frequency noise.

2. EXPERIMENTAL

Tunneling current spectrum measurements were performed with the use of a specially constructed experimental setup including both hardware and software parts, which was incorporated into a commercial ultra-high vacuum (UHV) room temperature STM Omicron system (base pressure $2\cdot10^{-11}$ Torr). The UHV system is decoupled from the building by a specially designed vibration isolation floor for optimal measurement conditions. In all the experiments, electrochemically etched tungsten tips were used. The STM tips were produced from tungsten wires (0.25 mm in diameter) that were electrochemically etched in 10 % KOH solution and cleaned in the UHV by flashing due to the direct current flowing. STM topographic images were obtained in the constant-current mode.

All the measurements were performed at room temperature. Before the beginning of any noise measurements, it was necessary to wait for more than 6 h to reach thermal equilibrium of the STM mechanical head to avoid thermal drift and ceramics crip. Thermal equilibrium was extremely important because the feedback loop was switched off during the noise measurements to prevent any spectrum changes caused by the STM electronics. Because we were interested in the frequencies lower than 1 Hz, an experimental run for one curve lasted for more than 100 s. Our main goal was to analyze how the tunneling contact parameters influence the value of the tunneling current noise spectrum, measured in the vicinity of localized surface states formed by the low-dimensional surface structures and surface defects. We performed tunneling current noise spectrum measurements in the vicinity of surface defects on a Si(111)–(7×7) surface and in the vicinity of one-dimensional structures on the Si(110)–(16×2) surface.

Si(111) samples doped by P were cut from the commercially available wafers. The doping concentration was $5\cdot10^{15}$ cm^{-3}. Si(110) samples were cut from the P-doped (110) oriented Si wafers with the nominal doping concentration about $5\cdot10^{16}$ cm^{-3}. Samples were ultrasonically cleaned in aceton and distilled water. With the use of "Ni-free" tools, they were mounted on the sample holder made from tantalum and degassed at 600 °C for 12 h. Further preparation of Si(111) surface deals with sample flashing at 1200 °C by direct current flowing and the subsequent slow sample cooling. Finally, the (7×7) reconstruction was obtained on the Si(111) surface. A typical STM image of the Si(111)–(7×7) surface reconstruction is shown in Fig. 1*a*. The STM-measured structure is consistent with the surface model of Si(111)–(7×7) suggested in [20]. After degassing, Si(110) samples were processed with argon-ion sputtering at 5 kV and 50 mA during 1 h. In the final stage of Si(110) surface preparation, samples were flashed at 1470 °C dy direct current flowing and slowly cooled down. A typical STM image of

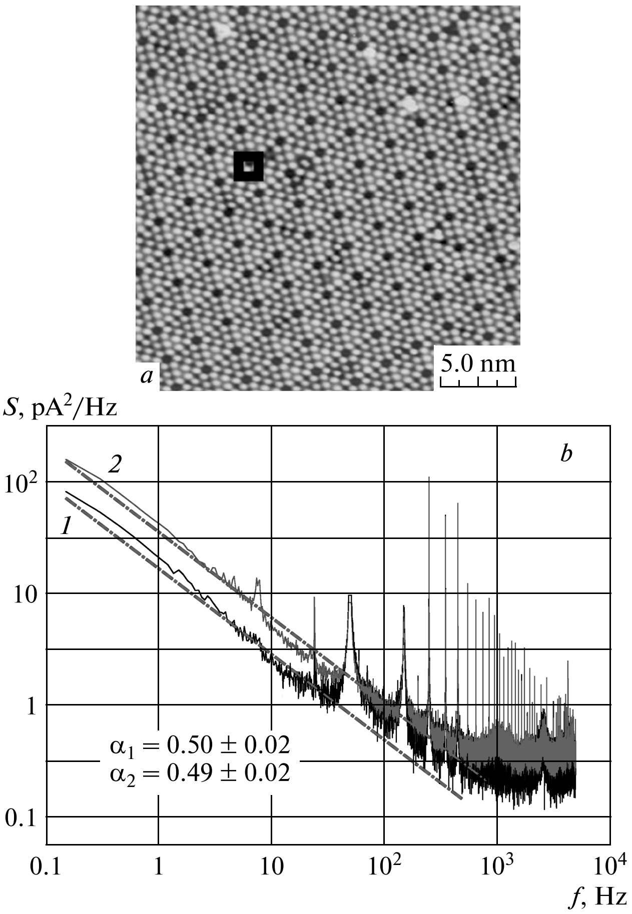

Fig. 1. *a*) STM image of Si(111)–(7×7) surface reconstruction. Scan area is 275×275 Å^2. Applied bias voltage $U_t = -1$ V, tunneling current $I_t = 50$ pA. The area that corresponds to the tunneling current noise spectrum measurements is marked by the black rectangle. *b*) Tunneling current noise spectra in the double logarithmic scale for different values of the tunneling current: *1* — $I_t = 25$ pA; *2* — $I_t = 100$ pA. Applied bias $U_t = -1$ V. Power-law exponent values are shown in the figure

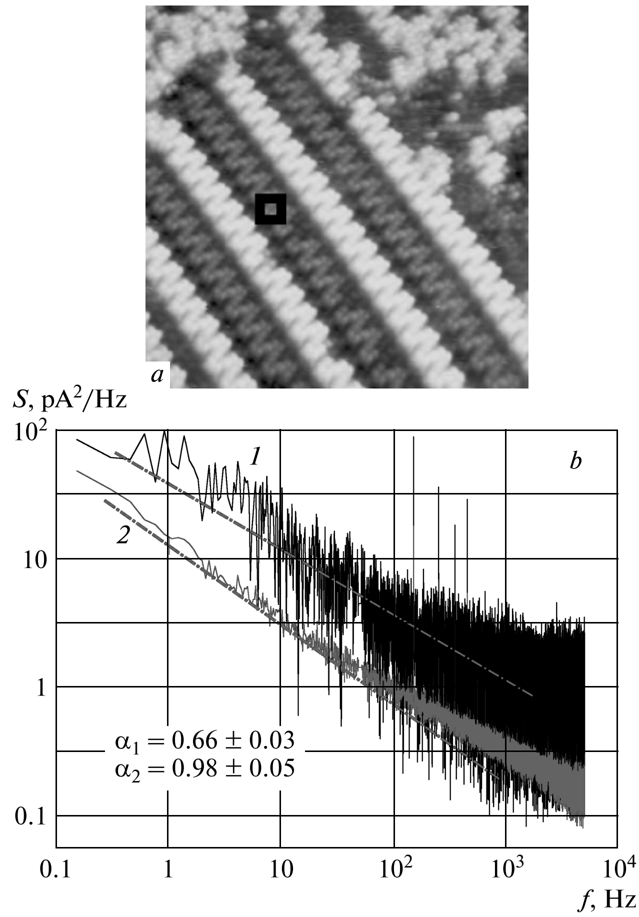

Fig. 2. *a*) STM image of Si(110)–(16×2) surface reconstruction. Scan area is 230×230 Å^2. Applied bias voltage $U_t = -1.5$ V, tunneling current $I_t = 50$ pA. The area that corresponds to the tunneling current noise spectrum measurements is marked by the black rectangle. *b*) Tunneling current noise spectra in the double logarithmic scale for different values of the applied bias voltage: *1* — $U_t = -0.7$ V; *2* — $U_t = 0.7$ V. Tunneling current $I_t = 25$ pA. Power-law exponent values are shown in the figure

Si(16×2) reconstruction on the Si(110) surface is presented in Fig. 2*a*. Areas with 5×1 reconstruction are also seen on the surface. The measured STM structure is consistent with the "pentagons" model of Si(110)–(16×2) surface reconstruction [21, 22].

The following experimental noise measurement procedure was used. After the sample preparation described above and the STM tip approach, it was necessary to wait for about 6 h to rich equilibrium tunneling conditions. Performed next were the search for an isolated defect on the Si(111) surface or a one-dimensional structure on Si(110) by means of STM imaging and acquisition of a high-resolution (5 nm × 5 nm) STM image of the corresponding part of the surface. The STM tip was positioned right above the defect or the one-dimensional structure on the surface with fixed values of the tunneling current and applied bias voltage. Because the relative displacement of the STM tip is small, the effects caused by manipulator ceramics creep are almost negligible, and hence only a few minutes are needed for stabilization. The feedback loop was interrupted for the time necessary to perform the tunneling current measurement, after which the feedback loop was switched on again. Finally, the control acquisition of a high-resolution (5 nm $\times$ 5 nm) STM image of the surface in the vicinity of the defect or the one-dimensional structure were performed to avoid any changes during measurements.

3. RESULTS AND DISCUSSION

We revealed in our previous paper [11] that there is a variation of the power-law exponent value in the vicinity of localized surface states in comparison with the measurements performed far away from surface-localized states. We revealed that the strongest effect occurs in the case where measurements are performed directly above the localized states. Our aim in this paper was to analyze the dependence of the power-law exponent of the low-frequency tunneling current noise spectrum on the tunneling system parameters. We consider that such analysis is mostly evident in the case where the effect is the strongest. This takes place when measurements are performed directly above the surface defects.

We start the discussion with the results obtained for the Si(111)–(7×7) surface. Tunneling current noise spectrum S measurements were performed above the surface area marked by the black rectangle in Fig. 1*a* and are shown in Fig. 1*b*. Curve *1* was measured with the tunneling current setpoint $I_t = 25$ pA and curve *2*, with $I_t = 100$ pA. The tunneling current setpoint is the value that continues being constant during the measurement procedure when the STM feedback loop is interrupted. The value of applied bias voltage was the same during both measurements and was equal to $U_t = -1$ V. It is evident from Fig. 1*b* that the shape of the tunneling current noise spectrum can be approximated in the best way by a $1/f^\alpha$ dependence. Deviations from this dependence become noticeable for the frequencies higher than 800 Hz. A fitting procedure gives the following values for the power-law exponents: $\alpha = 0.50 \pm 0.02$ for $I_t = 25$ pA and $\alpha = 0.49 \pm 0.02$ for $I_t = 100$ pA. The difference between the exponent values is lower than the experimental error. Consequently, it is possible to conclude that the tunneling current noise spectra are almost insensitive to the value of the tunneling current setpoint. The tunneling current value directly determines the distance between the surface localized state formed by the defect and the localized state on the STM tip. With an increase in the tunneling current, the distance decreases and stronger coupling between localized states takes place. Because we have not found the power-law exponent changes with the changing the tunneling current, we can conclude that the tunneling current noise spectrum amplitude does not depend on the coupling strength between the localized states in the tunneling contact.

Some additional noise (spikes) visible on the measured spectra are most probably due to the microphone effect and have no influence on the presented data. The dash-and-dot lines in Figs. 1*b* and 2*b* show the linear approximation of the current noise spectrum curve obtained by the least-mean-squares (LMS) method in the frequency range from 0.1 Hz to 1 kHz (the cutoff frequency). The power-law exponent was determined using several (at least 5) independent measurements in each case.

We also measured tunneling current noise spectra above the reconstructed Si(110)–(2×16) surface. Tunneling current noise spectrum measurements were performed above the surface area marked by the black rectangle in Fig. 2*a* and are demonstrated in Fig. 2*b*. The obtained results demonstrate a significant difference for the power-law exponent values measured for the different values of the applied bias: $\alpha = 0.66 \pm 0.03$ for $U_t = -0.7$ V and $\alpha = 0.98 \pm 0.05$ for $U_t = 0.7$ V. The difference is far above the experimental error level. We can explain such a strong difference between the obtained values of the power-law exponent as follows. When electrons tunnel from the sample valence band to the STM tip continuous-spectrum states, the overall dispersion of the tunneling current noise spectrum is a few times higher in comparison with the dispersion of the tunneling current noise spectrum for a positive value of the applied bias, when electrons tunnel from the STM tip continuum-spectrum states to the sample conduction band. This means that the power-law exponent value strongly depends on the electronic structure of the surface and, consequently, is determined by the relaxation rate values in the tunneling contact.

The obtained results correspond to the theoretical model proposed in [19], where the authors analyzed modifications of the tunneling current noise spectrum by the Coulomb interaction of conduction electrons in the leads with nonequilibrium localized charges in a tunneling contact due to the sudden switching on and off of localized-state Coulomb potentials during the electron tunneling processes.

4. CONCLUSION

We performed a detailed investigation of the tunneling current noise spectrum dependence on the tunneling contact parameters. We demonstrated that the power-law exponent strongly depends on the electronic structure of the sample and is independent of the value of the localized state coupling.

This work was partially supported by the RFBR (grant No. 13-02-91180), National Natural Science Foundation of China (grant No. 21203239), and NSFC grants under the contract № 21311120059 and was performed in cooperation with Wuhan Institute of Physics and Mathematics, Chinese Academy of Sciences.

REFERENCES

1. J. B. Johnson, Phys. Rev. **26**, 71 (1925).

2. R. F. Voss and J. Clarke, Nature **258**, 317 (1975).

3. R. J. Schoelkopf, P. Wahlgren, A. A. Kozhevnikov et al., Science **280**, 1238 (1998).

4. M. B. Weissman, Rev. Mod. Phys. **60**, 537 (1988).

5. Y. M. Lin and P. Avouris, Nano Lett. **8**, 2119 (2008).

6. Y. Zhang, E. E. Mandez, and X. Du, ACS Nano **5**, 8124 (2011).

7. G. Liu, S. Rumyantsev, M. Shur, and A. A. Balandin, Appl. Phys. Lett. **100**, 033103 (2012).

8. A. A. Kaverzin, A. S. Mayorov, A. Shytov, and D. W. Horsell, Phys. Rev. B **85**, 075435 (2012).

9. S. I. Park and C. F. Quate, Appl. Phys. Lett. **48**, 112 (1986).

10. E. Stoll and O. Marty, Surf. Sci. **181**, 222 (1987).

11. A. I. Oreshkin, V. N. Mantsevich, N. S. Maslova et al., Pis'ma v Zh. Eksp. Teor. Fiz. **85**, 46 (2007).

12. R. Moller, A. Esslinger, and B. Koslowski, Appl. Phys. Lett. **55**, 2360 (1989).

13. K. Maeda, K. Suzuki, S. Fujita, and M. Ichihara, J. Vac. Sci. Technol. B **12**, 2140 (1994).

14. M. Lozano and M. Tringides, Europhys. Lett. **30**, 537 (1995).

15. G. K. Zyrianov, *Low-Voltage Electronography*, Leningrad State Univ. Press, Leningrad (1986).

16. Yu. M. Galperin and K. A. Chao, Phys. Rev. B **55**, 12126 (1995).

17. L. S. Levitov and G. B. Lesovik, Pis'ma v Zh. Eksp. Teor. Fiz. **55**, 534 (1992).

18. B. L. Altshuler, L. S. Levitov, and A. Yu. Yakovets, Pis'ma v Zh. Eksp. Teor. Fiz. **59**, 821 (1994).

19. V. N. Mantsevich and N. S. Maslova, Sol. St. Comm. **147**, 278 (2008).

20. K. Takayanagi, Y. Tanishiro, S. Takahashi, and M. Takahashi, Surf. Sci. **164**, 367 (1985).

21. T. An, M. Yoshimura, I. Ono, and K. Ueda, Phys. Rev. B **61**, 3006 (2000).

22. N. S. Maslova, A. I. Oreshkin, S. I. Oreshkin et al., Pis'ma v Zh. Eksp. Teor. Fiz. **84**, 381 (2006).